Proceedings of the Institute of Acoustics

CALCULATION OF VIBRATION IN STRUCTURES

D E Newland and A Bhaskar
Cambridge University Engineering Department
Trumpington Street, Cambridge CB2 1PZ

1. SUMMARY

Research at Cambridge on building vibration includes analytical modelling of building and foundation response, laboratory measurements on structural damping, and field measurements at the Gloucester Park development in London. This paper discusses some analytical questions and includes some recent results from finite element studies and from idealisations of structural damping in a finite element model.

2. MODELLING

In order to study vibration transmission into and within resiliently mounted buildings, various models have been analysed. The simplest model is that of a uniform continuous column to represent the building, mounted on a massless spring and damper to represent the isolation pad. This has been examined in detail (Newland [6] ch.1) and the results show that transmissibility from the ground depends strongly on the dynamic characteristics of the building as well as on the properties of the isolation pads. A similar analysis by Grootenhuis [3] confirmed these conclusions. Various lumped parameter models have been studied by others, including Swallow [8] and Willford [9], and results from these have been used successfully in design. In 1988 we began to look at finite-element models of columns and frame structures (Wilson [10]) and we are now pursuing the finite-element approach in order to try to achieve closer agreement between theory and experiment. Our research group is also studying foundation dynamics in order to learn more about the ground excitation process and some aspects of that work are described by Hunt and Cryer [4] in their later paper.

Our finite-element analysis to date has concentrated on a two-dimensional model consisting of two vertical columns joined by two horizontal floors, fig.1. The parameter values are chosen so that the columns and the floors are all 30m long with the density and modulus of elasticity of concrete (2400kg/m^3 and 10^{10}N/m^2). The cross-sectional area of all the members is taken to be 1 m^2 and the radius of gyration for bending 0.282m. The floors are assumed to be integral with the columns and the feet of the two columns are mounted on resilient seatings. Both the seatings are represented by massless springs and viscous dampers in parallel and ground excitation is assumed to occur at the base of the right-hand seating only. Each resilient seating has stiffness of 230 MN/m and damping of 814 kNs/m. These values are chosen so that for a rigid column of the same mass as an actual column mounted alone on one seating, the natural frequency would be 9 Hz and the damping ratio 0.1. For the complete building, if it were rigid, the vertical natural frequency would be

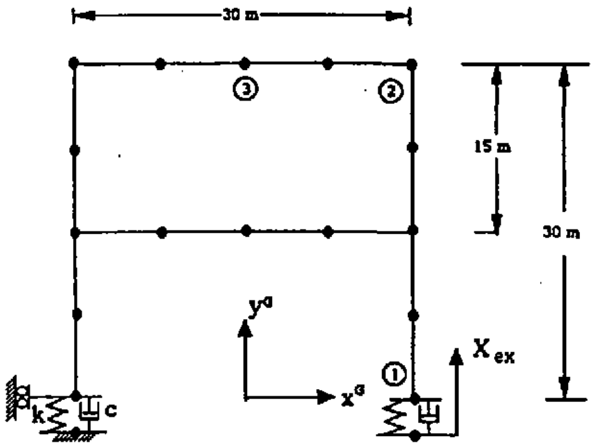

Figure 1: Two-dimensional frame structure with ground excitation at one point

$9/\sqrt{2} = 6.36$ Hz and the damping ratio $0.1/\sqrt{2} = 0.071$ because the complete building weighs twice that of the columns alone.

The finite element model needs a horizontal anchor (to remove a zero-frequency horizontal translational mode) and this is included by pinning the lower end of the left-hand column so that it is free to move vertically and to rotate, but its horiontal movement is prevented.

The elements that we have used allow axial compression and bending. Each element has two nodes (fig. 2), one at each end, and each node has three degrees-of-freedom which are the axial and transverse displacements and the in-plane rotation of the element at the node. In one model, we use 4 elements for each member (total 16 elements); in another model we use 8 elements for each member (total 32 elements). The mass and the stiffness matrices of each of the elements are given in the appendix. It is assumed that the distribution of displacement is linear in the axial direction and cubic in the transverse direction. These matrices are for generalised forces in the local coordinates of an element which are a lateral and transverse force at each node and a moment about an axis through the node perpendicular to the plane of the framework. The matrices are transformed to the global coordinate system (fig.3) using the geometrical transformations

$$\mathbf{M}_e^G = \mathbf{T}^t\mathbf{M}_e^L\mathbf{T} \tag{1}$$

$$\mathbf{K}_e^G = \mathbf{T}^t\mathbf{K}_e^L\mathbf{T} \tag{2}$$

where the subscript e refers to a typical element and the superscripts L and G refer to local and global coordinates respectively. $\mathbf{T}^t$ is the transpose of the transformation matrix $\mathbf{T}$

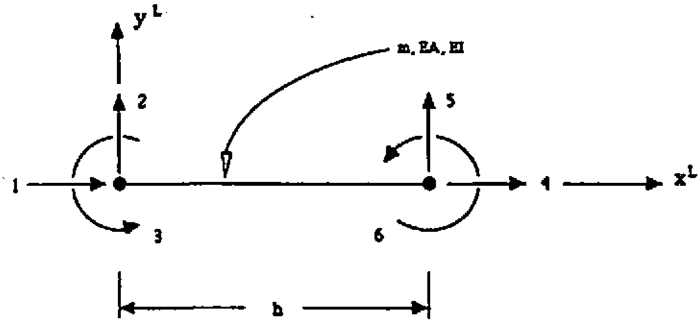

Figure 2: Nomenclature for the coordinates of a finite element with bending and compression.

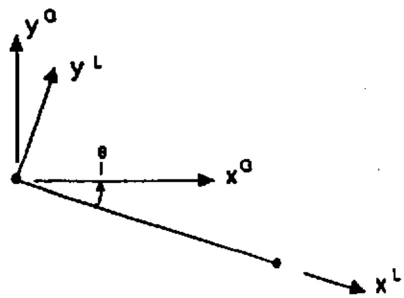

Figure 3: Relationship between local and global coordinates

given by

$$\mathbf{T} = \begin{bmatrix} \mathbf{t} & 0 \\ 0 & \mathbf{t} \end{bmatrix} \tag{3}$$

where

$$\mathbf{t} = \begin{bmatrix} \cos\theta & -\sin\theta & 0 \\ \sin\theta & \cos\theta & 0 \\ 0 & 0 & 1 \end{bmatrix}. \tag{4}$$

Since each of the elements has 6 degrees-of-freedom, all the element matrices have order 6×6. In order to introduce a damping matrix, we have assumed that there is Rayleigh damping so that

$$\mathbf{C}_e^{L/G} = \alpha \mathbf{M}_e^{L/G} + \beta \mathbf{K}_e^{L/G} \tag{5}$$

where C_e is the element damping matrix, L/G denotes either local or global coordinates, and α and β are constants. The numerical values taken for α and β are $\alpha = 21.375s^{-1}$ and

$\beta = 1.87 \times 10^{-4} s$. These are the same values as used for our column studies (Newland [6] ch.12). When $\alpha = 0$, the modal bandwidth increases in proportion to frequency squared. When $\beta = 0$, the modal bandwidth is constant.

We have found it convenient to model the resilient seatings as separate elements consisting of a discrete spring (stiffness k) and a damper (damping coefficient c) in parallel. The elemental stiffness and damping matrices are then

$$\mathbf{K}_e = \begin{bmatrix} k & -k \\ -k & k \end{bmatrix} \quad \text{and} \quad \mathbf{C}_e = \begin{bmatrix} c & -c \\ -c & c \end{bmatrix}. \tag{6}$$

If the two terminals of such a discrete element correspond to the i^{th} and the $(i+1)^{\text{th}}$ degrees-of-freedom of the global vectors, then

$$K_{ii}^G \leftarrow K_{ii}^G + k \tag{7}$$

$$K_{i,i+1} \leftarrow -k \tag{8}$$

$$K_{i+1,i} \leftarrow -k \tag{9}$$

$$K_{i+1,i+1} \leftarrow k \tag{10}$$

and similarly for the damping matrix. Two additional degrees-of-freedom are introduced by the resilient seatings. Where there are boundary conditions which constrain motion at the two nodes of the left-hand resilient seating, the appropriate rows and columns of the matrices and rows of the vectors are deleted. Hence the total number of degrees-of-freedom for our 16 beam element model is $16 \times 3 = 48$ plus 2 for the resilient seatings less two for the boundary constraints leaving 48 degrees-of-freedom altogether.

3. FREQUENCY RESPONSE TO GROUND EXCITATION

In this section some typical results are shown for the harmonic response of the model in fig. 1. They are expressed as transmissibilities with the magnitude of the harmonic response amplitude divided by the magnitude of the displacement amplitude at the lower side of the right hand resilient seating (see fig. 1). The equilibrium equations in the frequency domain can be expressed as

$$(-\omega^2\mathbf{M} + i\omega\mathbf{C} + \mathbf{K})\mathbf{X}(i\omega) = \mathbf{F}(i\omega) \tag{11}$$

where $\mathbf{M}, \mathbf{C}$ and $\mathbf{K}$ are the assembled mass, damping and stiffness matrices, $\mathbf{X}$ is the response vector and $\mathbf{F}$ is the external excitation vector. In order to compute transmissibility, all the entries of the force vector are zeros, except for the one corresponding to the ground excitation which receives a unit harmonic excitation. Because of the resilient seating, the global damping matrix turns out to be nonproportional after assembly of the elements. In order to compute the frequency response in such a situation without resorting to any assumptions, we invert the left-hand-side of equation (11) at every step of frequency so that the global response vector is given by

$$\mathbf{X}(i\omega) = (-\omega^2\mathbf{M} + i\omega\mathbf{C} + \mathbf{K})^{-1}\mathbf{F}(i\omega). \tag{12}$$

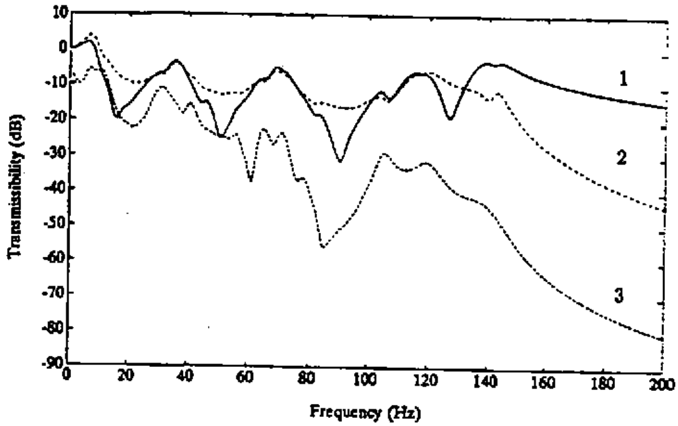

Figure 4: Transmissibility curves for the structure in fig. 1 for point 1 (the solid line), point 2 (the chain line) and point 3 (the dashed line) for the case when $\alpha = 21.375s^{-1}, \beta = 0$.

Transmissibility at the j^{th} degree-of-freedom is then obtained by scaling the response vector here with respect to the displacement computed at the ground excitation so that

$$T_j = 20\log_{10}\left|\frac{X_j}{X_{ex}}\right|. \tag{13}$$

In the following discussions, we present the results for two levels of discretisation. In the first model, the superstructure has been discretised into 16 elements; in the second one into 32. Transmissibilities for the first case at the base of the right-side column (above the resilient seating), top of the right-side column and middle of the top-floor span have been presented in fig. 4.

These results have been compared with results from a different model with a column alone on a resilient seating (Newland [6] ch.12). We notice that the general trends of transmissibility for the right-hand column agree fairly well with the responses computed from the column-alone model. This confirms that, for the level of complexity involved in the model in fig. 1, the right-hand side exhibits weak coupling with the rest of the structure as far as the vertical displacements are concerned. The mid-point of the top-floor-span, however, shows a different response and bears little resemblance with the top of the column. This is because the response of the horizontal member is dominated by bending. All the responses fall sharply after about 100 Hz on the frequency scale because higher natural frequencies are not included in the 16-element model. To study convergence the mesh was refined in the second model and the number of elements doubled to 32. With more degrees-of-freedom, new modes are exhibited after 100 Hz and the previously computed eigenfrequencies tend to go down, fig.5.

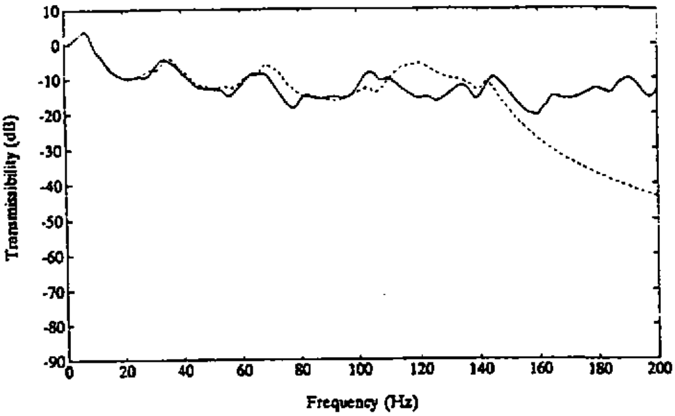

Figure 5: Transmissibility curves for point 2 of the structure shown in fig. 1 (the chain line) and for the same point when the frame is modelled by 32 elements (instead of 16). Damping is given by $\alpha = 21.375s^{-1}, \beta = 0$.

4. DAMPING ASSUMPTIONS

The main methods of calculating dynamic response are the direct integration method and the mode superposition method. The latter involves computing the response of each mode separately and then summing the response of all the modes of interest to obtain the overall response. For many problems this offers greater insight into the behaviour of the system being studied than direct integration.

For zero damping, the finite element model can be expressed as

$$\mathbf{M}\ddot{\mathbf{x}} + \mathbf{K}\mathbf{x} = \mathbf{f}(t) \tag{14}$$

where the n^{th} order response vector of displacements is $\mathbf{x}$ and the n^{th} order excitation vector is $\mathbf{f}(t)$. These n coupled equations can always be uncoupled by transforming to normal coordinates $\mathbf{q}$ to give

$$\ddot{\mathbf{q}} + \Lambda\mathbf{q} = \phi(t) \tag{15}$$

where Λ is a diagonal matrix whose elements are the natural frequencies squared (see e.g. Newland [6] p326). The coordinate transformation is

$$\mathbf{x} = \mathbf{U}\mathbf{q} \tag{16}$$

where $\mathbf{U}$ is the $n \times n$ matrix of the system's displacement eigenvectors (i.e. its normal modes).

This is for no damping and, if a damping matrix is not included in the finite element analysis, the equilibrium equations can can always be uncoupled by transforming to normal coordinates. However usually damping has to be included and the finite element model gives

$$\mathbf{M}\ddot{\mathbf{x}} + \mathbf{C}\dot{\mathbf{x}} + \mathbf{K}\mathbf{x} = \mathbf{f}(t). \tag{17}$$

Then the transformation to normal coordinates gives

$$\ddot{\mathbf{q}} + \mathbf{U}^t\mathbf{C}\mathbf{U}\dot{\mathbf{q}} + \Lambda\mathbf{q} = \phi(t) \tag{18}$$

and the equations will only be uncoupled if $\mathbf{U}^t\mathbf{C}\mathbf{U}$ is diagonal. If

$$\mathbf{C} = \alpha\mathbf{M} + \beta\mathbf{K} \tag{19}$$

then this will be so, but in general $\mathbf{U}^t\mathbf{C}\mathbf{U}$ will not be diagonal.

In order to simplify the finite-element analysis of structures, it is often assumed that the system's damping matrix satisfies (19). As mentioned already, for $\beta = 0$, so that each damping element is proportional to its corresponding mass element, it can be shown that all the modes have the same bandwidth. For $\alpha = 0$, when each damping element is proportional to its corresponding stiffness element, the modal bandwidth increases in proportion to frequency squared (Newland [6], p 336). For hysteretic damping, the damping term $\mathbf{C}\dot{\mathbf{x}}$ in (17) is replaced by $i\eta\mathbf{K}\mathbf{x}$ where η is the hysteretic damping factor. The resulting equation may only be used in the frequency domain. In this case, modal bandwidth increases in proportion to frequency for constant η although strictly it is not possible to hold η independent of frequency without violating the conditions of causality (see Newland [6], p 338). These conditions restrict the admissible forms of frequency response functions, which must be derivable from valid impulse response functions.

Although a combination of Rayleigh damping (a damping matrix satisfying equation (19)) and hysteretic damping will allow many continuous systems to be modelled satisfactorily, difficulty arises when localised sources of dissipation exist within assemblies of continuous systems. Then unless the ratio of damping to stiffness or damping to mass is the same as in the component continuous systems (which must all be the same in this respect) the combined system will not have a global damping matrix which is diagonal.

The mode superposition method is particularly effective if it can be assumed that there is Rayleigh damping, so that (19) applies, or that there is hysteretic damping, because then the free vibration mode shapes can be used as base vectors. Furthermore, numerical integration procedures can be applied to the motion in each uncoupled mode separately rather than integrating $2n$ first-order equations simultaneously (see for example, Bathe [1]). This may have considerable computational advantages.

We have therefore investigated procedures to approximate a non-diagonal damping matrix by an optimal diagonal damping matrix.

5. OPTIMAL DIAGONAL DAMPING MATRICES

We assume that equation (18) applies but that $\mathbf{U}^t\mathbf{C}\mathbf{U}$ is not a diagonal matrix. We want to replace it by a new diagonal matrix which allows the uncoupled equations to generate a solution vector $\mathbf{q}'(t)$ such that when transformed back to the physical coordinates by

$$\mathbf{x}'(t) = \mathbf{U}\mathbf{q}'(t) \tag{20}$$

gives an approximate solution vector $\mathbf{x}'(t)$ which is as close as possible to the exact solution vector $\mathbf{x}(t)$. Various alternative strategies can be pursued but we have approached the problem in the following way (Bhaskar [2]). Let the non-diagonal matrix $\tilde{\mathbf{C}}$ be written as

$$\mathbf{U}^t\mathbf{C}\mathbf{U} = \tilde{\mathbf{C}} = \mathbf{D} + \mathbf{R} \tag{21}$$

where $\mathbf{D}$ is diagonal and $\mathbf{R}$ therefore embraces all the off-diagonal elements in $\tilde{\mathbf{C}}$. Corresponding to (5), we then have

$$(\ddot{\mathbf{q}} + \mathbf{D}\dot{\mathbf{q}} + \Lambda\mathbf{q}) + \mathbf{R}\dot{\mathbf{q}} = \phi(t). \tag{22}$$

Since $\mathbf{D}$ and Λ are diagonal matrices, the equations would be uncoupled if $\mathbf{R}\dot{\mathbf{q}}$ were replaced by $\mathbf{A}\dot{\mathbf{q}}$ where $\mathbf{A}$ is diagonal. We choose $\mathbf{A}$ so that the sum of the squares of the differences between corresponding elements of $\mathbf{R}\dot{\mathbf{q}}$ and $\mathbf{A}\dot{\mathbf{q}}$ is as small as possible, which is so that

$$\int \|\mathbf{R}\dot{\mathbf{q}} - \mathbf{A}\dot{\mathbf{q}}\|^2 \mathrm{d}t = \text{a} \quad \text{minimum} \tag{23}$$

when the integral is evaluated over the time domain of interest. To do this, it is necessary first to solve for $\dot{\mathbf{q}}$ approximately from (22) after omitting the terms $\mathbf{R}\dot{\mathbf{q}}$.

In the minimisation (23), the unknowns are the elements of the diagonal matrix $\mathbf{A}$. Differentiating (23) with respect to a typical element A_{jj} gives

$$\frac{\partial}{\partial A_{jj}} \int \|\mathbf{R}\dot{\mathbf{q}} - \mathbf{A}\dot{\mathbf{q}}\|^2 \mathrm{d}t = 0 \qquad \textit{for} \quad j = 1 \quad \text{to} \quad n \tag{24}$$

which after some matrix algebra leads to the formula that

$$A_{jj} = \frac{\int (\sum_{k=1}^{n} R_{jk}\dot{q}_j\dot{q}_k)\mathrm{d}t}{\int \dot{q}_j^2 \mathrm{d}t}. \tag{25}$$

The elements $\dot{q}_j(t)$, $\dot{q}_k(t)$ come from the approximate solution vector $\dot{\mathbf{q}}$ obtained by solving (22) with the off-diagonal damping terms omitted (ie. with the term $\mathbf{R}\dot{\mathbf{q}}$ omitted). By differentiating (23) twice with respect to a typical diagonal element A_{jj}, it is found that the result is always positive, thus confirming that (25) always leads to a minimum (rather than a maximum) value for the integral in (23).

As an example, we consider the following three degree-of-freedom system which has been studied already by Shahruz [7].

$$\begin{bmatrix} 1 & 0 & 0 \\ 0 & 1 & 0 \\ 0 & 0 & 1 \end{bmatrix} \begin{Bmatrix} \ddot{q}_1 \\ \ddot{q}_2 \\ \ddot{q}_3 \end{Bmatrix} + \begin{bmatrix} 2.0 & -0.15 & -0.15 \\ -0.15 & 4.2 & -0.2 \\ -0.15 & -0.2 & 6.6 \end{bmatrix} \begin{Bmatrix} \dot{q}_1 \\ \dot{q}_2 \\ \dot{q}_3 \end{Bmatrix}$$

$$+ \begin{bmatrix} 4.0 & 0.0 & 0.0 \\ 0.0 & 4.41 & 0.0 \\ 0.0 & 0.0 & 9.0 \end{bmatrix} \begin{Bmatrix} q_1 \\ q_2 \\ q_3 \end{Bmatrix} = \begin{Bmatrix} 1 \\ 1.2 \\ 2.5 \end{Bmatrix} u(t) \qquad (26)$$

where $u(t)$ is a unit step function at $t = 0$ and the initial conditions of displacements and velocities are all zero at $t = 0$. Using the method described above, the matrix of the off-diagonal damping elements is

$$\mathbf{R} = \begin{bmatrix} 0 & -.15 & -.15 \\ -.15 & 0 & -.2 \\ -.15 & -.2 & 0 \end{bmatrix} \qquad (27)$$

and the computed replacement diagonal matrix **A** is

$$\begin{bmatrix} -.289 & 0 & 0 \\ 0 & -.283 & 0 \\ 0 & 0 & -.385 \end{bmatrix} \qquad (28)$$

This result has been obtained by calculating the $\mathbf{q}(t)$ response to substitute in (25) as the solution to (26) with the off-diagonal damping elements omitted and making the integration time in (25) run from $t = 0$ to $t = 15.0$ at which time the steady state response has been reached to a close approximation.

The computed response $\mathbf{q}$ when (26) is modified by replacing **R** by **A** is shown in fig. 6 alongside the exact response calculated by numerical integration of the 6 first-order equations to which the 3 second-order equations (26) may be reduced (see Newland [6] p.113). It is seen that there is very close agreement between the optimal response and the exact response. For comparison, the solution of (26) ignoring off-diagonal damping elements is also shown and has quite large errors at the response peaks. The same method can be used when the excitation is periodic, when the integration time in (25) has to be chosen to cover the time of transient settling and one or two periods afterwards. If greater accuracy is required, the method can be made iterative (Bhaskar [2]). After the replacement diagonal matrix **A** has been computed once, and the new approximate solution vector $\mathbf{q}(t)$ generated using **A**, the components of this vector can be used in (25) to compute a second approximation for **A** and hence a more accurate solution vector $\mathbf{q}(t)$.

6. FURTHER RESEARCH

So far the method of computing an optimal diagonal damping matrix has been applied only to test cases with a few degrees-of-freedom. Its application to large scale finite-element

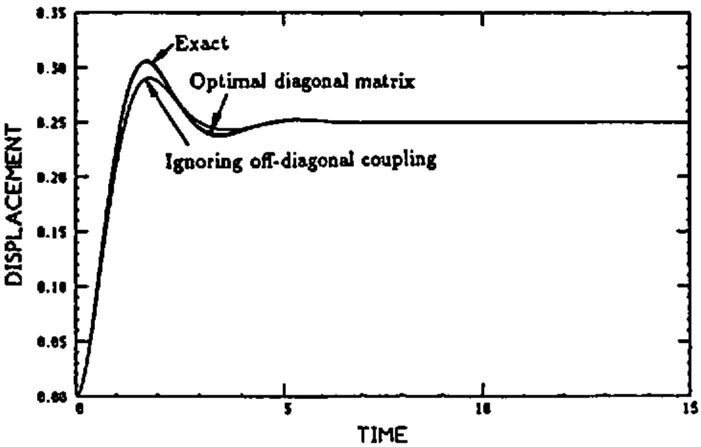

Figure 6: Computed step response of the system defined by equation 26 by three different methods

models with non-diagonal damping depends on the computational efficiency of the method. It may be possible to improve this by including within the summation in the numerator of (25) only those products $\dot{q}_j\dot{q}_k$ which make significant contributions to the integral; methods of identifying these are being studied.

Our next step is to model a simple real structure. We have in mind an acoustic damping chamber mounted on resilient bearings. The effect of the resilient bearings is expected to give a damping matrix with significant off-diagonal elements. Subsequently the intention is to apply this method to analysing the building under construction at Gloucester Road underground station in London, for which we hope to have good data. The experiments to determine this data are described in the companion paper by Hunt and Cryer [4].

References

[1] Bathe, K., Finite Element Procedures in Engineering Analysis, Prentice-Hall, Inc, New Jersey, 1982.

[2] Bhaskar, A., Some Studies on Damped Vibration of Linear Systems, Dissertation for Trinity College, Cambridge, 1990.

[3] Grootenhuis, P., Structural elastomeric bearings and resilient seatings. Chapter 9 of *Polymers and Polymer Composites in Construction*, Thomas Telford, 1989.

[4] Hunt, H. E. M. and Cryer, D. P., Site and Laboratory Experiments on Vibration Transmission, in this volume.

[5] Meirovitch, L., Elements of Vibration Analysis, Mc-Graw Hill, 1975.

[6] Newland, D. E., Mechanical Vibration Analysis and Computation, Longman, Harlow and John Wiley, New York, 1989.

[7] Shahruz, S. M., Approximate Decoupling of the Equations of Motion of Damped Linear Systems, *J. Sound Vib.*, 136(1), 51-64, 1990.

[8] Swallow, J. C., Modelling of isolation of buildings from ground-borne vibration, *Proc. 12th ICA, Canada*, D1-4, 1986.

[9] Willford, M. R., Personal communication, Ove Arup and Partners, London, 1990.

[10] Wilson. R. C., An investigation of vibration transmision through tall buildings. Cambridge University Engineering Department, Part II Project Report, 1988.

APPENDIX

The elemental mass matrix is given by (see Meirovitch [5] ch. 8)

$$\mathbf{M}_e = (mh/420)\begin{bmatrix} 140 & 0 & 0 & 70 & 0 & 0 \\ 0 & 156 & 22h & 0 & 54 & -13h \\ 0 & 22h & 4h^2 & 0 & 13h & -3h^2 \\ 70 & 0 & 0 & 140 & 0 & 0 \\ 0 & 54 & 13h & 0 & 156 & -22h \\ 0 & -13h & -3h^2 & 0 & -22h & 4h^2 \end{bmatrix}$$

where m is the mass per unit length of the element and h is the length of the element. The elemental stiffness matrix is given by

$$\mathbf{K}_e = (EI/h^3)\begin{bmatrix} r^2 & 0 & 0 & -r^2 & 0 & 0 \\ 0 & 12 & 6h & 0 & -12 & 6h \\ 0 & 6h & 4h^2 & 0 & -6h & 2h^2 \\ -r^2 & 0 & 0 & r^2 & 0 & 0 \\ 0 & -12 & -6h & 0 & 12 & -6h \\ 0 & 6h & 2h^2 & 0 & -6h & 4h^2 \end{bmatrix}$$

where r is the ratio of the length h to the radius of gyration r_g so that $r = h/r_g$.